On the effective optical fill factor of fine pitch metals

Anders Martensson (*), Bart Dierickx, Guy Meynants
Cypress/FillFactory, Schalienhoevedreef 20 B, 2800 Mechelen, Belgium
fbd@cypress.com, fgm@cypress.com
(*) Lund Institute of Technology, Lund University, Sweden

Abstract

CMOS pixels are covered by metal. This metal reflects part of the light directed on the pixel, thereby reducing the effective fill factor of the pixel. In the classic "ray tracing" approximation, the part of the pixel that becomes insensitive to light is exactly equal to the surface of the metallization. E.g., if one considers only the metal opacity, a stripe pattern with 50% metal and 50% openings has a "fill factor" of 50%. If we assume that the metal itself is not transparent this results in an average light attenuation of 50%.
This paper tackles questions such as: does this still hold when the metal stripe pitch becomes comparable to or less than the wavelength of the light, as is possible in present-day CMOS processes? What is the effective fill factor of two meshes of metal each having 50% coverage, lying on top of each other? And: can one cast this in design oriented rules-of-thumb?

1 Introduction

Today's CMOS fabrication processes realize nanometer scale. It has become possible to fabricate thinner and thinner metal wires, with dimensions far below the wavelength of visible light. How does the shrink affect the fill factor of CMOS image sensors? More precisely, can a metal area in a pixel still be considered as opaque in the classical sense?
This paper investigates the transmission of a dense metal mesh in a typical CMOS image sensor context. The transmission of periodical nano-apertures has got attention lately and many papers have been published both on experimental results[1,2] and different simulation approaches[3]. Current CMOS pixel dimensions have not yet reached the nano-aperture realm but are clearly in the sub-wavelength range where linear optics does not longer apply.
Electromagnetic simulation (section 2) was used to simulate the optical transmission of different metal line configurations. The results are presented in sections 3 and 4. As a practical result of this research, in section 6, a rather 'qualitative' or 'intuitive' approach is proposed as guideline for pixel designers to estimate the effective optical dimensions of metal lines, rather than using the full numerical or analytic approach.

2 EM simulations

Electromagnetic (EM) simulations were used to determine the effective fill factor of the metal lines. A commercial software package (Microwave Studio from CST) based on the finite integration technique (FIT) is used to solve Maxwell's equation. The FIT is based on solving Maxwell's equations on the integral form[4] and then use a time-step approach to solve the EM equations for a transient problem in the time domain.
The simulations were performed on 2D cross-sections of infinitely long metal lines embedded in Silicon dioxide. The oxide was modeled as an ordinary dielectric while the three different models were used: the perfect electrical conductor (PEC), the semi-perfect metal (SPM) and the Drude model. The Drude dispersion model was used for the majority of simulations while a semi-perfect metal material (featuring a one-dimensional surface loss model) was used for the larger simulation decks. The perfect electric conductor is too simplistic for small structures and was disregarded from the beginning. The Drude model is supposed to be more accurate than the semi-perfect metal. Their differences should be more important for small metal dimensions when the penetration depth of the EM wave is no longer negligible.

In a typical simulation, the structure is excited by a plane wave (being a Gaussian pulse) running from top to bottom through the simulation space. The transient response is calculated, transformed to the frequency domain, and Poynting vector is extracted. The vertical Poynting vector component is used to determine the effective transmission: the integrated power flow over a line at the bottom end of the simulation domain is calculated. For calibration of the 100% transmission point, a reference is always made to a simulation space containing only SiO2.

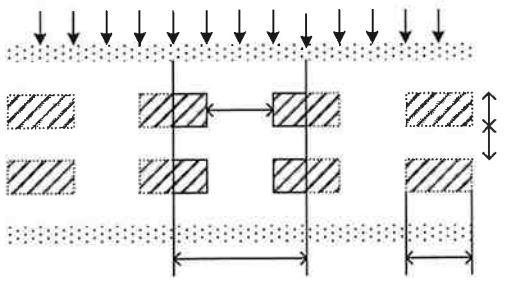

Figure 1 Simulated structure including two metal layers. The oxide thickness is the same (0.35μm) in all simulations. The actual simulation domain is marked in the figure and periodic boundary conditions are applied to create an infinite, periodic structure

Perfectly matched layer (PML) boundary conditions were applied in the vertical direction while periodic boundaries were used in the horizontal direction modeling the periodic structure (fig. 1).

3 The transmission of regular metal grids

The periodic structure in fig. 1 was simulated for different light polarizations and increasing line&spacing width *w*. To isolate the *w* dependence for a periodic structure, a one-layer structure was simulated. The transmission results for green light (λ=540nm) are shown in fig. 2. The polarizing effect of the grid for S-polarized light (E-field vector parallel to the metal line extension) predicted by the EM theory is clearly seen as the S-polarized light is cut off around $\lambda/2$. Wire grid polarizers have been used in CMOS image sensors by e.g. Catrysse and Wandell[5].

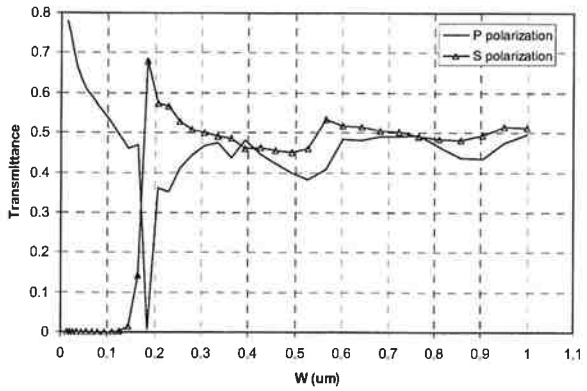

Figure 2. Transmittance for green light (540nm) vs. metal width *w* through one layer of periodic metal lines

The P-polarized light (electric field vector perpendicular to metal lines) have high transmission also below $\lambda/2$. The dependence on *w* for two metal lines on top of each other (c.f. figure 1) is shown in fig. 3.

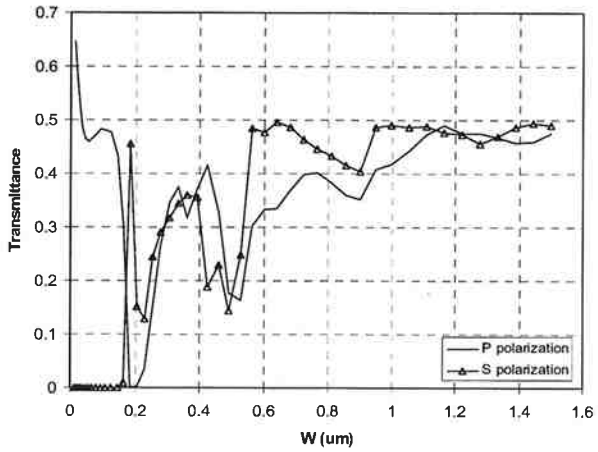

Figure 3 Light transmission through double layers of metal lines (c.f. fig. 1) versus *w*. Green light (540nm) and both polarizations shown

The single layer simulations shows oscillations and a transmission peak near $\lambda/2$ which is attributed to resonances in the 'cavities' between the metals, consistent with previous observations[6]. Transmission through the double metal layer shows the same basic oscillating behavior, but also an attenuation caused by the double-layer is observed. The transmission approaches 50% when *w* is large, converging towards the classical limit. The transmission results reach very high values when *w* is in the 25 nm range. It should be noted that it is not sure if the Drude model used is still valid for these extremely small dimension. With the advent of nanometer technologies, such dimensions will become realistic.

It is also possible that the simulation set-up also inflict some issues. In any case, the results at very small *w* should be interpreted with a large grain of salt.

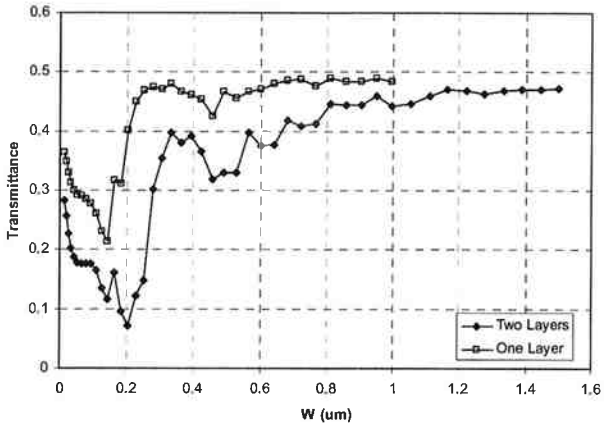

Figure 4. Average transmittance fro green light (540 nm) averaged over both polarization for one and two layers of metal

4 Metal line variations

In this section we study and report simulations on variations on the theme in section 3.

Multiple layers

The effect of having multiple layers stacked on top of each other was investigated, based on same configuration shown in fig. 1, only more layers were stacked on top of each other.

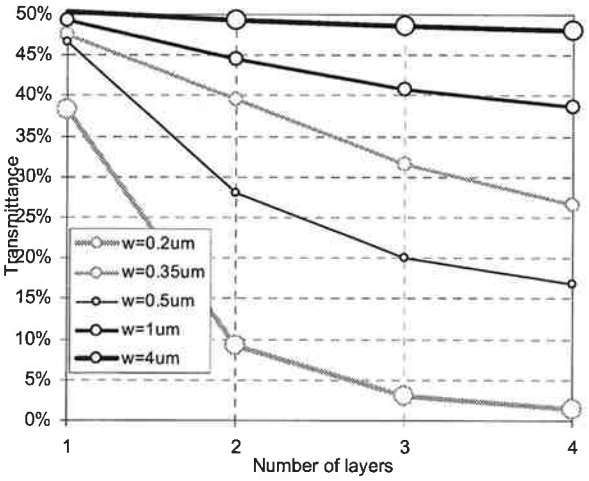

Figure 5 Transmittance versus number of layers for a regular mesh. Metal thickness 0.25um, separation 0.35um. The graph shows the average over red, green, blue and both polarization directions.

The structures were simulated for different openings w and results can be found in fig. 5. The transmission for 3 and 4 layers confirms the trend observed for the two-metal case: the 'cavity' effects of the horizontal periodicity are enveloped by attenuation by the increasing number of layers.

Shifted metals

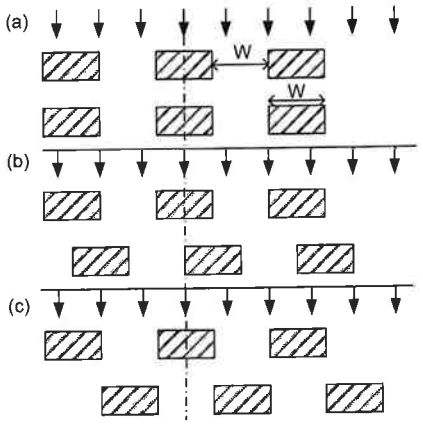

Figure 6 Two-layer structures, lower layer shifted in respect to upper. (a) 0° shift (b) 90° shift (c) 180° shift

A set-up with two metal layers was simulated, having the second layer shifted horizontally in respect to the top layer (figure 6). Transmission results are shown in fig. 7. The average transmission is higher than expected for w less than 1μm for the shifted layers. This might be attributed to diffraction and reflections that counteract the shift of the metals. The transmission goes towards the values expected from ray optics for $w > 1$μm. The transmission is still >0 for the 180° shift even at higher w in contrast to the classical solution.

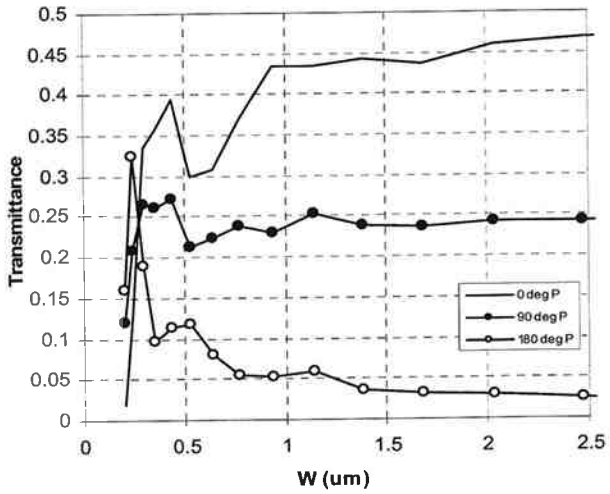

Figure 7 Transmission through two layers, lower layer shifted in respect to upper layer (fig. 6). Average transmission over red, green and blue light and P polarization versus w

Single lines/apertures

A set of simulations was performed to study thin lines with wide spacing. Structures similar to the multilayer cases were used, cfr. fig 8. The metal lines had a spacing of 6μm and periodic boundary conditions were used to ensure that all the scattered light would eventually be accounted for. The effective optical widths for a line of typical thickness are plotted vs. the geometrical width in fig.9. No important effective width change is noticed for lines far apart while the effect is pronounced for periodic meshes, and even more for multiple layers of meshes, consistent with the overall resonance behavior.

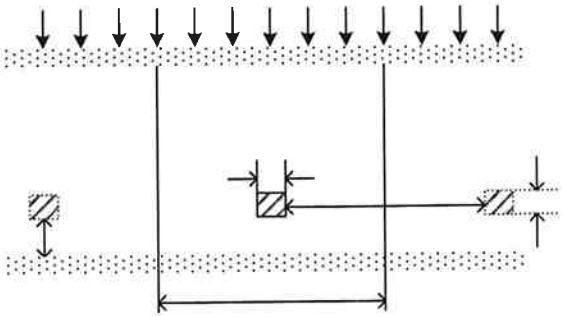

Figure 8 Single lines width wide spacing. The distance between lines is 6μm and periodic boundary values was used

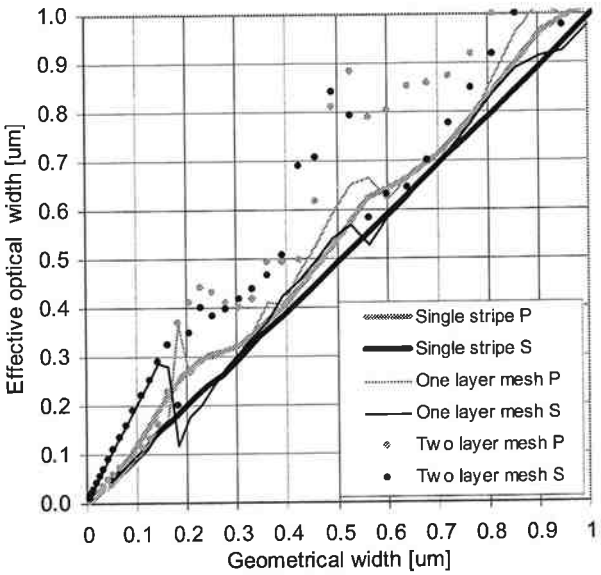

Figure 9 Effective optical width versus geometric line width: a single stripe, a periodic mesh and a two layer periodic mesh with 0.35μm layer separation. Metal thickness was 0.25μm for all cases. P and S polarization.

Similarly, the effective optical aperture is plotted vs. the geometrical aperture in fig.10.

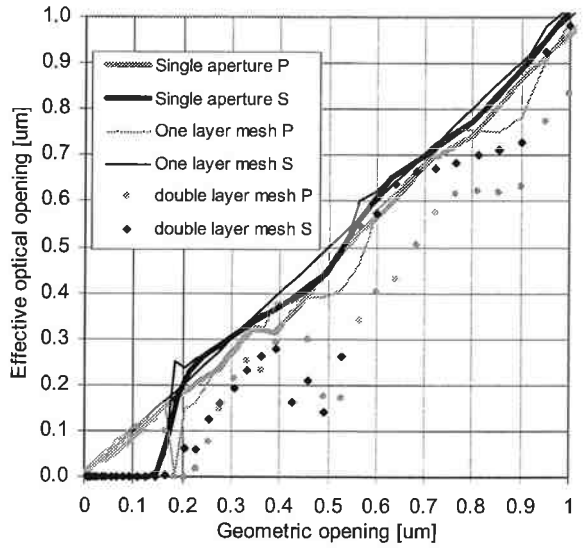

Figure 10 Effective optical opening versus geometric opening: a single gap, a periodic mesh and a two layer periodic mesh with 0.35μm layer separation. Metal thickness 0.25μ

Metal thickness

The thickness of the metal layer can influence the transmission for a given stripe width w. A number of simulations were carried out for a mesh of lines in a single layer (c.f. fig. 1), keeping the width and spacing w constant while varying the thickness t. The same thickness sweep was simulated for the widely spaced lines in fig. 8; the effective optical width vs. metal thickness can be found in fig 11. The optical width increases in a linear fashion both for the periodical and the widely spaced lines. The effective optical width is larger than the geometrical width for all configurations except when w is extremely small.

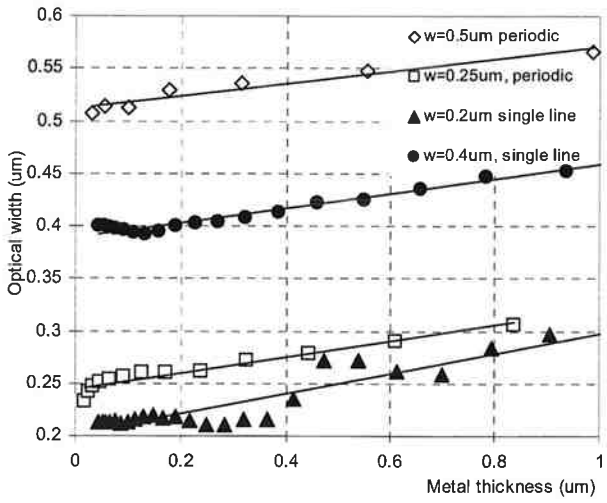

Figure 11 Effective optical widths versus metal thickness, averaged over RGB and both polarizations. The full lines are straight line fitted to the simulated data.

5 Review of the metal models

The metal model used has clear influence on the simulation results. The Drude dispersion is considered as a good approximation of the dielectric properties of good conductors such as Aluminum. The differences with more trivial models become important when the metal dimensions are small. A series of simulations was performed varying w of single metal layer of periodic stripes (same as in section 3) for PEC, Drude and the semi-perfect metal model. A comparison is shown in fig. 12. All the three models are converging to the same results for $w > 1\mu m$. This is consistent with the assumptions. Some differences are noted for small w, probably because the part of the field penetrating the metal becoming increasingly important. The difference is smaller between the different models for the S polarization, maybe explained by the deeper penetration for P-polarized light.

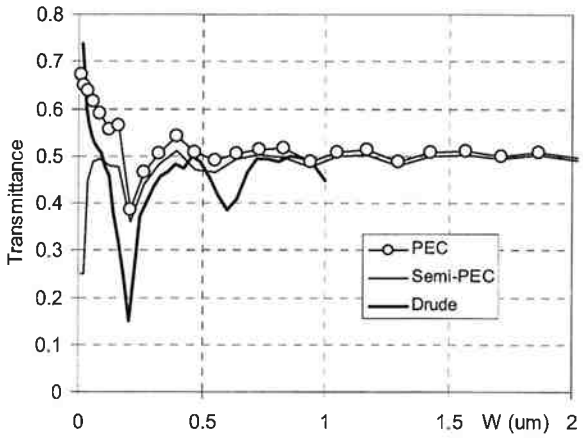

Figure 13 Metal model example: Transmittance of P-polarized green light (540 nm) through a periodic mesh of metal lines. One metal layer 0.25μm thick.

6 Pixel design guidelines

In a practical design application, we do not want to spend exhaustive simulations efforts to optimize pixel layouts for optimal transmission through the metal routing.

The results of this elementary research allow us to propose a few rules of thumb that may help us to design better metal routing.

(1) P or S polarized lines behave significantly different. One models realistic light as a 50% / 50% mix.

(2) Details on wavelength (spectral) behavior are difficult to cast in a rule of thumb. This is especially true for metal spacings and metal layer separations in the range $\lambda/2$ to λ.

(3) The effect of the thickness of the metal, i.e. the absorption through homogenous slabs, is accounted for separately,.

(4) Thin lines with large spacings appear slightly wider. The increase is in the order or $\lambda/8$ to $\lambda/4$.

(5) Thin slits in wide metal slabs appear slightly smaller. All transmission ceases abruptly for S-polarization if the slit is smaller than $\lambda/2$.

(6) Closely spaced metal lines, where the spacing is equal to the metal width, appear roughly as wide as they are for P-polarization, and are about $\lambda/2$ wider for S-polarization.

(7) Multiple layers on top of each other behave as the projected superposition of the behavior of single layers. At least - this applies for wide lines and

spacings, and layer separation that is not close to λ/2. When the line width and spacing comes in the order of the wavelength, one should take into account that each metal mesh layer "scrambles" the wave front: EM radiation will not behave as ray traces; a lower metal cannot hide in the shadow of a higher metal. The severity of this scrambling depends also on the thickness of the intermetal dielectric.

(8) The thickness of the metal layers, apart from the plain classic absorption, affects the apparent optical width. For orthogonal light, when the stripes are spaced wider than the wavelength, it seems that the optical width increases by about 7% of the thickness. For spacings thinner than λ/2, this does not hold; S-polarized light will be blocked unless the layers are really thin; P-will penetrate better. For illumination under an angle, one should assume that the light sees the projected side walls.

7 Conclusions

The effect on visible EM wave transmission through periodic metal lines in different configurations was simulated using the Finite Integration Technique. Effective optical transmission was calculated and large deviations from ray-tracing predictions were observed.

As fabrication processes become successful in creating even smaller patterns, the design task become hard as our intuitive feeling about fill factor and other optical issues will not hold anymore.
The effects of different configurations were summarized as far as possible in rules-of-thumb for a pixel layout designer.

The trends for the smallest dimensions simulated should be interpreted with care, mainly because of doubts on the material parameters and the validity of the models for extremely thin metals.

[1] S.C. Hohng, Y.C. Yoon, D.S. Kim, V. Malyarchuk, R. Müller, Ch. Lienau, J.W. Park, K.H. Yoo, J. Kim, H.Y. Ryu, Q.H. Park, "Light emission from the shadows: Surface plasmon nano-optics at near and far fields", Appl. Phys. Lett. **81**, 3239 (2002)
[2] C.H. Wei, P.H. Tsao, W. Fann, P-K Wei, J.O. Tegenfeldt, R.H. Austin, "Polarization dependence of light intensity distribution near a nanometric aluminum slit", J. Opt. Soc. Am. B 21, **1005** (2004)
[3] J. Olkkonen, K. Kataja, J. Aikio, D.G. Howe, "Study of high throughput aperture for near field optical data storage", Technical digest, ODS 2003, Vancouver 2003 (conference paper)
[4] R. Marklein in W. R. Stone (ed.), *Review of Radio Science: 1999-2002 URSI*, (IEEE Press and John Wiley and Sons, Piscataway and New York, 2002) pp. 201-244.
[5] P.B. Catrysse, B.A. Wandell, "Integrated color pixels in 0.18-μm complementary metal oxide semiconductor technology", J. Opt. Soc. Am. A **20**, 2293 (2003)
[6] M.A. Jensen, G.P. Nordin, "Finite-aperture wire grid polarizers", J. Opt. Soc. Am. A **17**, 2191 (2000)